Available online at www.sciencedirect.com

ScienceDirect

International Journal of Pharmaceutics 352 (2008) 152–158

INTERNATIONAL JOURNAL OF PHARMACEUTICS

www.elsevier.com/locate/ijpharm

Thermal behavior of water in the selected starch- and cellulose-based polymeric hydrogels

Damrongsak Faroongsarng [a,*], Patchara Sukonrat [b]

[a] Drug Delivery Systems Research Center, Department of Pharmaceutical Technology, Faculty of Pharmaceutical Sciences, Prince of Songkla University, Hat Yai 90112, Thailand
[b] Scientific Equipment Center, Prince of Songkla University, Hat Yai 90112, Thailand

Received 13 June 2007; received in revised form 30 August 2007; accepted 21 October 2007
Available online 26 October 2007

Abstract

In a polymer–water matrix, freezable water is depressed due to either porosity confinement or interaction. The aim of the study was to examine water crystallization/melting depression by sub-ambient differential scanning calorimetry. The selected starch- and cellulose-based polymers including pre-gelatinized starch (PS), sodium alginate, sodium starch glycolate, hydroxypropylmethyl cellulose (HPMC), sodium carboxymethyl cellulose, and croscarmellose sodium were employed. The pre-treated with ambient humidity (85–100% relative humidity, at 30.0 ± 0.2 °C for 10 days) and with excess water (hydrogels) samples were subjected to between 25 and −150 °C cooling–heating cycle at 5.00 °C/min rate. The volume fractions of hydrogels were measured by light scattering technique. It was observed that all polymers but PS and HPMC with ambient humidity presented freezable water in two distinct fractions namely bound water where crystallizing/melting temperature was depressed and bulk water. The water transition in samples with various contents exhibited the pattern as a polymer solution, thus rather than confinement, the depression was due to interaction. The volume fraction-melting temperature data derived from endotherms of hydrogels were successfully fitted to Flory's model (r^2: 0.934–0.999). The Flory's interaction parameters (χ_1) were found to vary between 0.520 and 0.847. In addition, the smaller the value of χ_1, the larger melting was depressed, i.e., stronger affinity for water.

Keywords: Freezable water; Water–polymer interaction; Flory's interaction parameter (χ_1); Melting point depression; Hydrogel

1. Introduction

Starch- and cellulose-based materials derived from naturally occur biopolymers are the major pharmaceutical excipients utilized in drug delivery dosage forms. These polymers always interact with water due to their hydrophilicity exhibiting some properties that may critically affect the dosage form performance. For example: in controlled release devices, water diffusion through a polymeric hydrogel layer has been considered as one of the major factors determining drug release rate (Rajabi-Siahboomi et al., 1996). With liquid water in excess, these hydrophilic polymers could form hydrogels, i.e., the three-dimensional arrangement possessing the ability to retain a significant fraction of water without complete dissolving. A hydrogel might form relatively stable space lattice or network pores fulfilled with a considerable amount of water. The interfacial tension related to surface of curvature of water within pores could develop and affect the phase transition of the water. Thus this phase transition of water confinement could somehow characterize the pores where it occupies. A number of authors, for examples: Yamamoto et al. (2005), Faroongsarng and Peck (2003), Hay and Laity (2000), and Ishikiriyama and Todoki (1995) examined the pore sizes and distributions of various porous materials assuming that water is mostly held within pores, with melting temperature being depressed by Gibbs–Thomson effect. However, the depression of melting temperature is not only attributed by water confinement in porosity but the water–polymer interaction. Rault et al. (1995) reported that the melting depression and the concentration of unfrozen water varied with the water concentration with similar orders of magnitude for polymer–water systems and simple binary mixtures, presenting the same type of interaction, from which

---

[*] Corresponding author. Tel.: +66 74 288 841; fax: +66 74 428 148.
E-mail address: damrongsak.f@psu.ac.th (D. Faroongsarng).

0378-5173/$ – see front matter © 2007 Elsevier B.V. All rights reserved.
doi:10.1016/j.ijpharm.2007.10.022

confinement effects are absent. They concluded that the melting depression is due not to water confinement in polymer network porosity but rather to water–polymer interactions. The evidence was later confirmed by the work of Okoroafor et al. (1998).

In general, interactions between macromolecules fall into four categories: ionic, hydrophobic, van der Waals and hydrogen bonding (Ilmain et al., 1991). But for a polymer–water mixture, the interaction is always in the range of hydrogen bonding. It has been proposed (Ping et al., 2001; Zografi and Kontny, 1986; Higuchi and Iijima, 1985) that water in hydrophilic polymer matrices presents in three distinct fractions: (i) non-freezable bound water, (ii) freezable bound water, and (iii) free or bulk water. Upon cooling, water begins to crystallize only when its content is above a characteristic threshold. This fraction of water has been called freezable bound water (fraction (ii)) because it exhibits a melting point lower than 0 °C which is distinguished from bulk water and it should correspond to the depression phenomenon described above. In the lower-than-threshold level, i.e., the water of fraction (i), the molecules of water interact with polar functional groups such as carboxyl groups on polymer chains. The interaction would be well-oriented hydrogen bonding which is locally favorable configuration that being strong enough to prevent water to form ice crystals (Ping et al., 2001). The differential scanning calorimetric (DSC) study can reveal the freezable water fractions, for example: Nakamura et al. (1981) reported two DSC peaks of crystallization of absorbed water on celluloses including a broad peak observed at ∼230–250 K and a sharp one at ∼255 K. Should the melting depression of water of fraction (ii) be due to polymer–water interaction, the corresponding DSC peak then could describe the thermodynamics of a polymer–water system. Many techniques are available for the experimental determination of the interaction parameter between solvent molecules and the polymeric chain segment. However, the methods were usually based on volumetric determinations (Mantovani et al., 2000). The melting/freezing depression determined by DSC could also exhibit the great potential to characterize that interaction. The aim of the study is to examine the thermal behavior of water melting depression due to its interaction with the selected starch- and cellulose-based polymers commonly used in drug delivery formulations by mean of DSC technique.

2. Materials and methods

2.1. Materials

The variety in nature of starch- and cellulose-based polymers including pre-gelatinized potato starch (PS: Starch®1500, Colorcon, Inc., PA, USA), sodium alginate (SA: Wendt-Chemie, Hamburg, Germany), sodium starch glycolate (SSG: Explotab®, JRS Pharma, Rosenberg, Germany), hydroxypropyl methyl cellulose (HPMC: Colorcon, Inc., PA, USA), sodium carboxymethyl cellulose (SCMC: Wendt-Chemie, Hamburg, Germany) and croscarmellose sodium (CCS: Ac-di-sol®, FMC Corp., PA, USA) were employed. SA, PS, and SSG were charged-linear, branch and linear, and charged cross-linked polysaccharides, respectively. HPMC, SCMC, and CCS were linear, charged-linear, and charged cross-linked celluloses, respectively.

2.2. Samples preparations

The samples were pre-treated with ambient humidity prior to DSC analyses. The ∼5-g samples were equilibrated with 85%, 96%, and 100% relative humidity (RH) at 30.0 ± 0.2 °C for 10 days. The samples were also fully hydrated by liquid water in excess at the same temperature as those pre-treated with ambient humidity as follows: A 3- to 8-g sample (equivalent to approximately 10-ml bulk volume) was thoroughly mixed with liquid water to 100 ml in volume. The mixtures were allowed to be still for 1 day. Hydrogels or sediments depending to the nature of water–polymer mixtures were subjected to sub-ambient differential scanning calorimetric study. The total water (W_T) contents of hydrogel/sediment samples were determined using a moisture balance (Metter® LP16 & PM300, Metter-Toledo, Inc., Hightstown, NJ, USA) with heating temperature of 100 °C.

2.3. Sub-ambient differential scanning calorimetric study

The Perkin-Elmer differential scanning calorimeter (DSC7 with TAC7/DX Thermal analysis controller, Perkin-Elmer Crop., Norwalk, CT, USA) equipped with liquid nitrogen bath set as a cooling accessory was employed. Calibrations with indium and cyclohexane were carried out for every time which the DSC operation started to ensure the accuracy/precision of the obtained heat of transitions and the corresponding temperatures. An accurately weighed (5–15 mg) sample was placed in tightly sealed aluminum pan (Perkin-Elmer Crop., Norwalk, CT, USA). The samples were subjected to run against an empty pan as a reference. With loading temperature of 25 °C, the analysis program includes (1) cooling from 25 to −150 °C at 5.00 °C/min rate, (2) isothermal run at −150 °C for 1 min, and (3) heating from −150 to 25 °C at the same rate as cooling step. The distilled water was run to validate the temperature and heat of water crystallization/melting. All of DSC thermograms (cooling or heating traces) were analyzed using Pyris® software (Perkin-Elmer Crop., Norwalk, CT, USA).

2.4. The determination of non-freezable water

The water of fraction (i) was calculated by subtracting the total water content (W_T) by the water content calculated from the amount of heat corresponded to DSC melting traces in sub-ambient temperatures assuming that the area of melting peak of pure water corresponds to the melting enthalpy. So, the heat was converted to the amount of water since it was directly proportional to enthalpy of melting obtained from DSC tracing of distilled water.

2.5. The determination of polymer volume fraction in liquid water

The fully hydrated polymer volume fraction (ϕ_{2V}) was obtained from particle size determination in non-swelling and swelling states, as analogous to what was done previously (Mantovani et al., 2000). The size and distribution of each of the polymeric powders were measured by dynamic laser light scattering technique (Mastersizer®/E, Malvern Instruments Ltd., Worcestershire, UK). Alcohol and water were used as non-swelling and swelling media, respectively. ϕ_{2V} was obtained by comparing mean volume diameters according to the equation of $\varphi_{2v} = [\bar{d}_{\mathrm{al}}/\bar{d}_{\mathrm{w}}]^3$, where $\bar{d}_{\mathrm{al}}$ and $\bar{d}_{\mathrm{w}}$ are geometric mean volume diameters of a powdered polymer in alcohol and in water, respectively.

To quantify the polymer volume fraction during ice-liquid phase transition of water denoted by ϕ_2, it was assumed that only pure water freezes when cooled to freezing point. ϕ_2 is thus directly proportional to the cumulative partial area under the DSC peak at corresponding T, i.e., $\varphi_2 = \varphi_2^{(i)} - \Lambda(A_T/P)$, where $A_T, P, \varphi_2^{(i)}$, and Λ are the area under the peak at temperature T, the total area under the peak, the polymer volume fraction with water of fraction (i), and the linear coefficient that makes ϕ_2 equals ϕ_{2V} determined by light scattering technique, in which A_T equals P, respectively. $\varphi_2^{(i)}$ was approximated from mole fraction of water of fraction (i) ($x_1^{(i)}$) calculated based on the water content of non-freezable water previously described, i.e., $\varphi_2^{(i)} \approx (1 - x_1^{(i)})$. The ϕ_2 and its corresponding T were non-linearly fitted into Flory's model using the commercial software (SigmaPlot® 2000, SPSS, Inc.).

3. Results and discussion

3.1. In situ water crystallization: the validation of DSC measurement

The cooling and heating traces revealing water crystallization and melting, respectively, are in Fig. 1. There was an exothermic peak of water crystallization (I in Fig. 1) occurred at a temperature far below 0 °C. Endothermic melting peak (II in Fig. 1), on the other hand, started at a normal melting temperature. This inconsistency between freezing and melting curves is commonly observed in fairly slow rate of scanning (1–10 °C/min). It is because the crystallization difficulty causes an exotherm to appear at a temperature lower than normal. It seems that the melting trace could approach an equilibrium ice-water transition better than cooling counterpart as the tracing was close to 0 °C.

Table 1
Water melting information taken from endotherm (heating trace) compared with the reference (Dean, 1985)

Parameter	DSC run	Reference (l)	Deviation (%)
Onset; peak (K)	274.15; 275.4	273.15	+0.37; +0.82
Heat of melting (kcal/mol)	1.453	1.436	+1.18

The thermal reference data including onset and enthalpy of melting of pure water calorimetrically determined according to the methods described by National Institute of Standard and Technology, US Department of Commerce (former name: *National Bureau of Standard*) were taken from Dean (1985). The detailed information of water melting in the current study compared with this reference (Dean, 1985) was tabulated in Table 1. As seen in Table 1, both onset and heat of melting for pure water agree with the values taken from the reference. Very low deviations, i.e., 0.37% and 1.18% deviate from reference values for onset and heat of melting, respectively, are observed. It has been stated that in typical DSC measurement, the mean error at heating/cooling rate of 1–10 °C/min should not exceed 2.5% (Borchard et al., 2005). Thus, the method and its conditions could be used to investigate water crystallization/melting with acceptable precision and accuracy.

3.2. DSC water tracings in the selected hydrophilic polymers and the nature of ice-liquid water transition

Fig. 2 illustrates the tracings of water that could be found in SA, SSG, SCMC, and CCS equilibrated with ambient humidity (85–100% RH). For simplicity, the only tracings of SA-100%

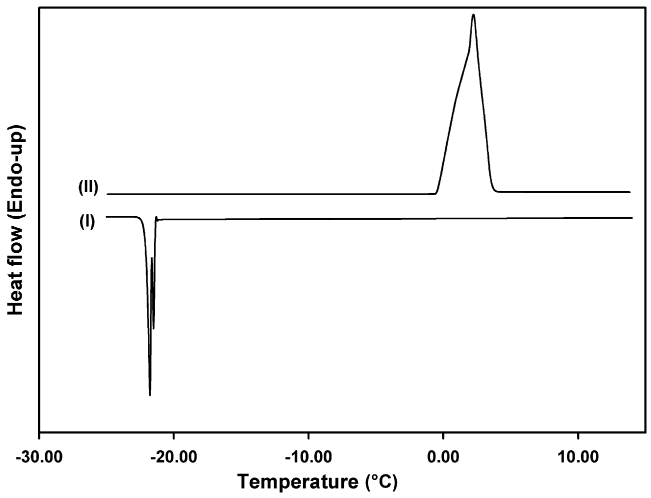

Fig. 1. DSC thermograms of water illustrating water crystallization (cooling trace: I) and melting (heating trace: II). DSC was done according to the conditions listed in Table 1.

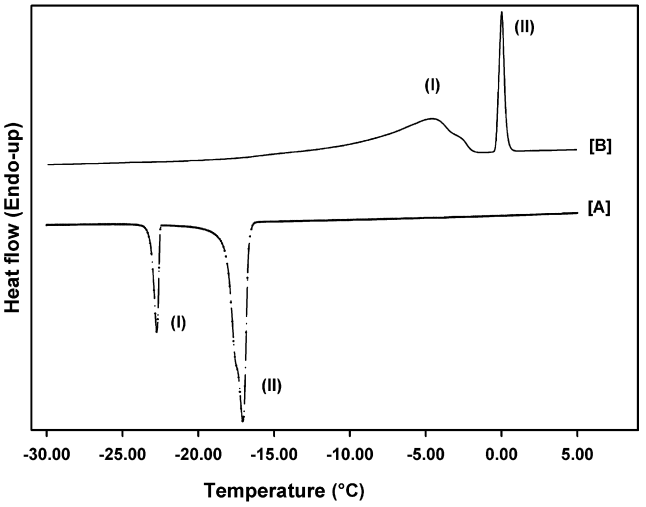

Fig. 2. DSC thermograms (cooling (A) and heating (B) curves) of SA previously equilibrated in 100% RH at 30 °C for 7 days showing two phases of water on a polymer surface. (I) is freezable bound water and (II) is bulk water.

RH system are showed. As seen in Fig. 2, the freezable water in current study is consistent with previous report (Nakamura et al., 1981). It is then subjected into two fractions, i.e., water of fraction (ii) labeled as (I) where freezing/melting happen at a temperature below zero, and that of fraction (iii) labeled as (II) where its transitions are closed to normal melting point. Fig. 3 illustrates the DSC freezing traces of CCS with various aqueous level environments including that with liquid water in excess. It is noted that other polymers in this study showed similar patterns. However, the water transition tracings were absent in the cases of PS and HPMC in ambient humidity but fully hydrated samples. PS and HPMC are non-ionic polymers exhibiting less hygroscopic than others. It may be because ionic species and salts could attribute to hydration on polymer they present with and might allow amount of water uptake greater than threshold of non-frozen water to show the DSC tracings of water of fraction (ii) and (iii) in cases of SA, SSG, SCMC, and CCS.

If the porosity formed by three-dimensional polymer network should govern the freezing/melting point depression, then the depressed temperature in various moisture environments of the same polymer, which would form similar pore structures might be invariant. Furthermore, if the pores collapse during ice formation, the transition of water of fraction (ii) might be either near or far from that of water of fraction (iii) dependent on the new size of the pores that water occupies after collapsing. As obviously showed in Fig. 3, there are not the cases in the present study. It is observed that the phase transition of water of fraction (ii) always exhibits a pattern as a polymer solution, i.e., the more concentration level of water; the more freezing temperature is depressed. Thus rather than porosity confinement, the freezing temperature may be depressed in accord with polymer–water interaction.

Fig. 4 illustrates the endothermic melting traces of SSG with variety of humidity as well as fully hydrated sample. Like freezing exotherms, the melting endotherms of various level of water with polymer samples under study were also in similar patterns. It is observed that the melting of freezable bound water shifts toward the melting of free water, i.e., the two singlet peaks turn to a doublet with increase in water content which is similar to the previous study (Borchard et al., 2005). It may be because water of fraction (ii), during increasing temperature, becoming liquid phase migrates from the vicinity of polymer interaction sites within gel due to hydrogen bonding among water molecules to be in equilibrium again with free water that melt later at a normal melting temperature.

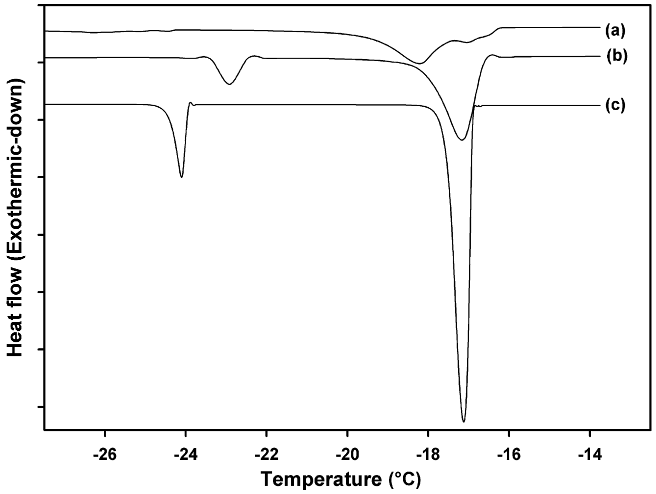

Fig. 3. DSC freezing traces of water in the samples of CCS equilibrated with (a) 96% RH, (b) 100% RH, and (c) liquid water. It is noted that hydrogels of other polymer under study also exhibit similar behavior.

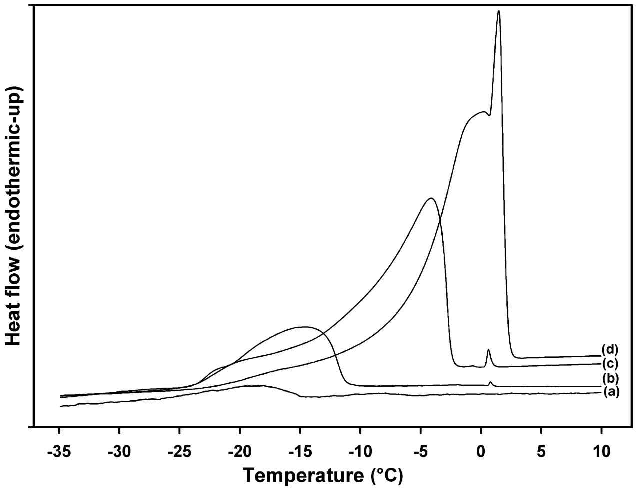

Fig. 4. DSC endothermic melting of ice in SSG equilibrated with (a) 84% RH, (b) 96% RH, (c) 100% RH, and (d) excess liquid water (fully hydrated). It is noted that hydrogels of other polymer under study also exhibit similar behavior.

3.3. Non-freezable bound water

An attempt at the determination of water of fraction (i) for each of polymer–water systems was made and tabulated in Table 2. The materials under study exhibit the non-freezable water contents of between 9.67% and 26.63% whereas it was previously reported that starches and celluloses exhibited non-freezable bound water contents of 28% (Zhong and Sun, 2005) and 22–25% (Luukkonen et al., 2001), respectively. McCrystal et al. (1997) estimated the number of moles of non-freezing water per a polymer repeating unit for HPMC gel as approximately 3.8 mol that is corresponding to approximately 10–20% water content dependent on degrees of substitution, while the current study on HPMC is within the range (13.21%, Table 2). On the other hand, the cross-linked chemically modified starch and cellulose that are more hygroscopic (SSG and CCS) illustrate low level of non-freezable bound water (Table 2). It might be because these materials present more number of ice nuclei, during freezing, that draw more water molecules due to hydrogen bonding to the ice clusters as a process of lowering surface free energy. As a result more portion of freezable water may be detected.

3.4. The volume fraction of polymeric hydrogels vs. melting depression: non-linear fitting to the Flory's model

The volume fractions in liquid water (φ_{2V}) of fully hydrated polymers under study are tabulated in Table 2. It is noted that φ_{2V}

Table 2
Water contents and the volume fractions of fully hydrated hydrophilic polymers under study

Polymeric material	Overall water content (%)[a]	Freezable water content (%) (mean, S.D.)[b]	Water of fraction, (i) (%)[c]	φ_{2V}[d]
PS	80.01	53.38, 1.09	26.63	0.112
SA	73.36	47.43, 1.07	25.93	0.167[e]
SSG	73.28	52.30, 1.11	20.98	0.031
HPMC	51.30	38.09, 0.87	13.21	0.384[e]
SCMC	69.13	46.14, 0.78	22.99	0.145
CCS	79.97	70.30, 1.11	9.67	0.054

[a] Overall water content was determined by moisture balance.

[b] Freezable water content was determined by DSC traces calculation (in three replicates) based on the heat of melting in Table 1.

[c] Non-freezable water content was calculated as overall water content minus freezable water content.

[d] The fully hydrated polymer volume fraction based on equation (Mantovani et al., 2000): $\varphi_{2V} = [\bar{d}_{\mathrm{al}}/\bar{d}_{\mathrm{w}}]^3$ where $\bar{d}_{\mathrm{al}}$ and $\bar{d}_{\mathrm{w}}$ are geometric mean volume diameters of a powdered polymer in alcohol and in water, respectively.

[e] The numbers are taken from reference (Mutalik et al., 2006) since the equipment could not determine.

of SA and HPMC have been taken from the reference (Mutalik et al., 2006) since the polymers dissolved in water and alcohol, respectively. φ_{2V} of sodium starch glycolates have been previously reported as the numbers between 0.005 and 0.045 (Mantovani et al., 2000) whereas φ_{2V} of SSG, which is chemically identical, is 0.031 (Table 2). In addition, the DSC melting traces yield the endotherms closed to 0 °C compared to the exotherms of freezing traces (Figs. 2 and 4). Thus the endothermic melting transition of a fully hydrated polymer is used in order to have an appropriate φ_2.

3.5. The thermodynamic relations for a polymer solution: Flory's model

A general thermodynamic theory of polymer solution based on mixing according to liquid lattice theory has been presented by Flory (1971). For polymeric hydrogels employed in the present study, the chemical potential of water (μ_1) in a water–polymer system includes not only Flory's mixing with swollen gel but the Donnan equilibrium for polyelectrolytes that yields the following relationship (Flory, 1971; Okoroafor et al., 1998; Mantovani et al., 2000; Ozmen and Okay, 2005; Borchard et al., 2005):

$$\mu_1^{\mathrm{gel}} - \mu_1^0 = RT[\ln(1-\varphi_2) + \varphi_2 + \chi_1\varphi_2^2 + V_1\left(\frac{\upsilon_{\mathrm{e}}}{V_0}\right)(\varphi_2^{1/3} - \varphi_2^2) - f\varphi_2] \quad (1)$$

where φ_2, χ_1, υ_{e}, and f are volume fraction of polymer in gel, the Flory's polymer–water interaction parameter, the effective cross-link density of the network, and the fraction of charged units in the hydrogel network, respectively. V_1 and V_0 are molar volume of water and the volume of relaxed hydrogel network. R and T are gas constant and absolute temperature. μ_1^0 is the chemical potential of pure liquid water. And, μ_1^{gel} is the chemical potential of water in hydrogel. The first three terms in the right hand side of Eq. (1) represent the chemical potential of general polymer–water mixture. The fourth term is the chemical potential due to reaction of the network cross-link structure (Flory, 1971), whereas the last term is that from Donnan equilibrium theory (Mantovani et al., 2000; Ozmen and Okay, 2005).

It is further assumed that frozen water is in equilibrium with the unfrozen water in gel phase during the DSC operation, i.e., the chemical potential of freezing ice (μ_1^{ice}) and of water in hydrogel (μ_1^{gel}) must be equal. And when a mixture freezes, one of the colligative properties known as freezing point depression holds. The change of chemical potential can be written as (Ozmen and Okay, 2005):

$$\mu_1^{\mathrm{ice}} - \mu_1^0 = \Delta H_{\mathrm{m}}\left(\frac{T}{T_0} - 1\right) \quad (2)$$

Where ΔH_{m}, and T_0 are molar enthalpy of crystallization (or melting), and melting temperature of pure water, respectively. Since the left hand side of Eqs. (1) and (2) are equal, the arrangement of these two equations yields:

$$\frac{1}{T} = \frac{1}{T_0} - \frac{R}{\Delta H_{\mathrm{m}}}[\ln(1-\varphi_2) + \varphi_2 + \chi_1\varphi_2^2 + V_1\left(\frac{\upsilon_{\mathrm{e}}}{V_0}\right)(\varphi_2^{1/3} - \varphi_2^2) - f\varphi_2] \quad (3)$$

This equation should be applicable to the water of fraction (ii) where the ice-liquid water transition temperature was depressed. And, assuming the involved parameters are constant over the transition temperature, the parameters such as χ_1 could be obtained by non-linear regression of $1/T$ as a function of φ_2 according to the model described by Eq. (3).

Each of φ_2–T data sets derived from DSC curves was non-linearly fitted into Eq. (3) with the restricted conditions that $(R/\Delta H_{\mathrm{m}}) = 1.383 \times 10^{-3}\ \mathrm{K}^{-1}$ and $T_0 = 273.15\ \mathrm{K}$ (Borchard et al., 2005). The estimates as well as their standard errors (S.E.) of parameters including χ_1, network factor ($V_1(\upsilon_{\mathrm{e}}/V_0)$) and f are tabulated in Table 3. It is noted that ionic and/or cross-linking network contribution factor was set as null for uncharged and/or linear polymers, respectively. It was found that the model is successfully applied to φ_2–T data sets with high correlations (r^2: 0.934–0.999, Table 3). It is thus demonstrated that χ_1, charges, and polymer network affect the crystallization/melting of water that the polymer contains. As see in Table 3, f of charged polymers are statistically significant from null at α-level of 0.05, so are network factors of cross-linked ones except CCS. f reflects the degree of ionization whereas network factor illustrates swelling of the cross-linked polymers (Borchard et

Table 3
The estimates of the parameters according to the restricted ($R/\Delta H_m = 1.383 \times 10^{-3}\,K^{-1}$ and $T_0 = 273.15$ K) non-linear regression of Eq. (3)

Polymeric material	χ_1 estimate, S.E.	$V_1\left(\frac{v_e}{V_0}\right)$ estimate, S.E.	f estimate, S.E.	r^2
PS	0.761, 0.041	0.067, 0.017	–[b]	0.939
SA	0.738, 0.033	–[a]	0.513, 0.022	0.986
SSG	0.520, 0.051	0.084, 0.010	0.288, 0.093	0.994
HPMC	0.847, 0.032	–[a]	–[b]	0.934
SCMC	0.776, 0.021	–[a]	0.368, 0.070	0.947
CCS	0.679, 0.025	[c]0.028, 0.048	0.241, 0.002	0.999

[a] Since the polymers are linear, network contribution is absent.
[b] Since the polymers are uncharged, the reduced model with $f = 0$ is used.
[c] The contribution is statistically non-significant at 0.05 α-level.

al., 2005; Mantovani et al., 2000). It is observed that at 0.05-α-level, network factor in the case of CCS is not significantly different from null. It might evidently be because the swelling of the polymeric network is not sufficient to significantly effect on the water crystallization/melting for it was previously reported that the swelling capacity of CCS present in water was far lower than that of SSG (Visavarungroj and Remon, 1990). In addition, Okoroafor et al. (1998) mentioned that the effect of network factor was quite small since its value usually is of the order of two decimal digits. That is consistent with the current study as it is observed that the estimates of network factor are in the same order of magnitude (Table 3).

3.6. Flory's interaction parameter (χ_1)

To characterize the thermodynamic interaction between water and polymer, Flory (1971) introduced a dimensionless quantity: χ_1. It represents merely the difference in energy divided by thermal agitation energy (kT: where k is Boltzmen's constant) of a solvent molecule immersed in the pure polymer compared with one surrounded by molecules of its own kind. A number of authors reported the magnitudes of χ_1 of aqueous polymeric solutions including starches and its derivatives (Baks et al., 2007; Cruz-Orea et al., 2002; Mantovani et al., 2000; Farhat and Blanshard, 1998), and sodium alginate (Borchard et al., 2005) as the numbers ranging between 0.43 and 0.67. As seen in Table 3, the estimates of χ_1-parameters of the same types of polymers vary between 0.520 and 0.761, which are comparable. Myagkova et al. (1997) mentioned that the χ_1 should be approximately 0.5 for maximum dissolving capacity of liquid water, i.e., the good-solvent conditions, for cellulose esters whereas the magnitudes of χ_1 for the same type of polymers under study are 0.679–0.847 which also approaches those conditions. In fact, the magnitude χ_1 is somewhat empirical and not a constant. It is dependent on volume fraction as well as temperature (Myagkova et al., 1997; Flory, 1971). Thus experimental conditions should affect its magnitude especially during the initial setting causing χ_1 values to deviate from laboratories to laboratories.

Fig. 5 illustrates the plot of χ_1 versus the reciprocal absolute temperature of the onset of DSC melting transition of water of fraction (ii) in fully hydrated samples. It is observed that the smaller the value of χ_1, the larger solvent water melting was depressed, i.e., stronger affinity for water. Flory (1971) rectified the energy quantity of χ_1 that should be regarded as the free energy change rather than as the heat of mixing only. χ_1 then contains an entropy contribution in addition to enthalpy one. Thus, in a simple case (Borchard et al., 2005):

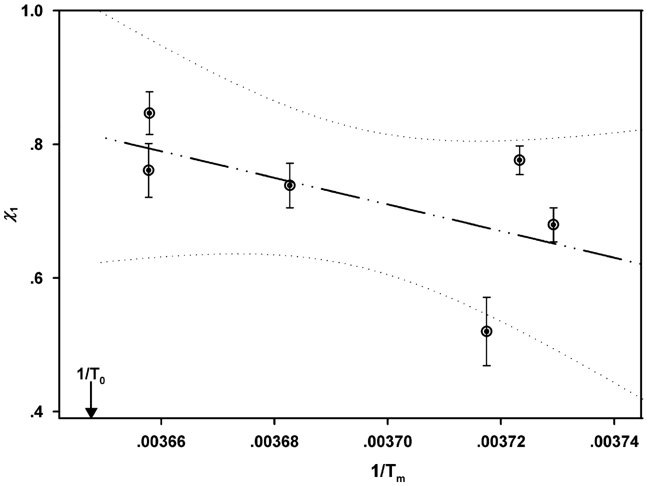

Fig. 5. The plot of χ_1-parameter against the reciprocal of onset temperature (in absolute scale) of melting transition of freezable bound water in water–polymer systems under study.

$$\chi_1 = \alpha_1 + \frac{\beta_1}{T} \tag{4}$$

where α_1 and β_1 are entropy and enthalpy parameters, respectively. Assuming the same type of interaction, χ_1 derived from polymeric hydrogels in this study could exhibit the relationship with $1/T$ as showed by Eq. (4). As seen in Fig. 5, the trend line as well as 95% confidence interval (dotted lines in Fig. 5) represents the data fitting of Eq. (4). Unfortunately, the power of regression and the correlation coefficient are as low as 25.01% and 0.631%, respectively. It might be because the variety in nature of individual polymers and experimental conditions could complicate the systems resulting the fitted parameters are so empirical that they are meaningless to address.

4. Conclusion

The water transition in starch- and cellulose-based polymeric hydrogels under study behaved as a polymer solution. Thus, its freezing depression was due to polymer–water interaction rather than water confinement in hydrogel porosity. The volume fraction-melting temperature data derived from DSC endotherms of water in the hydrogels were successfully fitted to Flory's model of polymer solution with very high correlations. The Flory's interaction parameters (χ_1) were found to vary between 0.520 and 0.847. In addition, the smaller the value of χ_1, the larger melting was depressed, i.e., stronger affinity for water.

Acknowledgements

The authors would like to thank Thailand Research Fund and Commission on Higher Education for financial support. Special thanks also go to the Scientific Equipment Center, Prince of Songkla University; Faculty of Pharmaceutical Sciences' Research and Development Unit; and the Department of Pharmaceutical Technology, Faculty of Pharmaceutical Sciences, Prince of Songkla University, for providing the lab facilities.

References

Baks, T., Ngene, I.S., van Soest, J.J.G., Janssen, A.E.M., Boom, R.M., 2007. Comparison of methods to determine the degree of gelatinisation for both high and low starch concentrations. Carbohyd. Polym. 67, 481–490.

Borchard, W., Kenning, A., Kapp, A., Mayer, C., 2005. Phase diagram of the system sodium alginate/water: a model for biofilms. Int. J. Biol. Macromol. 35, 247– 256.

Dean, J.A., 1985. Lange's Handbook of Chemistry, 13rd ed. McGraw-Hill, New York, pp. 9–117.

Cruz-Orea, A., Pitsi, G., Jamee, P., Thoen, J., 2002. Phase transitions in the starch-water system studied by adiabatic scanning calorimetry. J. Agric. Food Chem. 50, 1335–1344.

Farhat, J.A., Blanshard, J.M.V., 1998. On the extrapolation of the melting temperature of dry starch from starch-water data using the Flory-Huggins equation. Carbohyd. Polym. 34, 263–265.

Faroongsarng, D., Peck, G.E., 2003. Thermal porosity analysis of croscarmellose sodium and sodium starch glycolate by differential scanning calorimetry. AAPS Pharm. Sci. Technol. 4 (Article 67).

Flory, P.J., 1971. Principles of Polymer Chemistry. Cornell University Press, Ithaca and London.

Hay, J.N., Laity, P.R., 2000. Observation of water migration during thermoporometry studies of cellulose films. Polymer 41, 6171–6180.

Higuchi, A., Iijima, T., 1985. DSC investigation of the states of the water in poly(vinyl alcohol) membranes. Polymer 26, 1207–1211.

Ilmain, F., Tanaka, T., Kokufuta, E., 1991. Volume transition in a gel driven by hydrogen bonding. Nature 349, 400–401.

Ishikiriyama, K., Todoki, M., 1995. Pore size distribution measurements of silica gels by means of differential scanning calorimetry. J. Colloid Interf. Sci. 171, 103–111.

Luukkonen, P., Maloney, T., Rantanen, J., Paulapuro, H., Yliruusi, J., 2001. Microcrystalline cellulose-water interaction—a novel approach using thermoporosimetry. Pharm. Res. 18, 1562–1569.

Mantovani, F., Grassi, M., Colombo, I., Lapasin, R., 2000. A combination of vapor sorption and dynamic laser light scattering methods for the determination of the parameter χ and the cross-link density of a powdered polymeric gel. Fluid Phase Equilibr. 167, 63–81.

McCrystal, C.B., Ford, J.L., Rajabi-Siahboomi, A.R., 1997. A study on the interaction of water and cellulose ethers using differential scanning calorimetry. Thermochim. Acta 294, 91–98.

Mutalik, V., Manjeshwar, L.S., Wali, A., Sairam, M., Raju, K.V.S.N., Aminabhavi, T.M., 2006. Thermodynamics/hydrodymanics of aqueous polymer solutions and dynamic mechanical characterization of solid films of chitosan, sodium alginate, guar gum, hydroxyl ethyl cellulose and hydroxypropyl methylcellulose at different temperatures. Carbohyd. Polym. 65, 9–21.

Myagkova, N.V., Rakhmonberdiev, G.R., Sagdieva, Z.G., Sidikov, A.S., 1997. Thermodynamic properties of solutions of water-soluble mixed cellulose esters. Chem. Nat. Compd. 33, 76–79.

Nakamura, K., Hatakeyama, T., Hatakeyama, H., 1981. Studies on bound water of cellulose by differential scanning calorimetry. Text. Res. J. 51, 607–613.

Okoroafor, E.U., Newborough, M., Highgate, D., Augood, P., 1998. The thermal behavior of water in cross-linked hydroactive polymeric structure: crystasllization of water. J. Phys. D: Appl. Phys. 31, 3120–3129.

Ozmen, M.M., Okay, O., 2005. Polymer 46, 8119–8127.

Ping, Z.H., Nguyen, Q.T., Chen, S.M., Zhou, J.Q., Ding, Y.D., 2001. States of water in different hydrophilic polymers-DSC and FTIR studies. Polymer 42, 8461–8467.

Rajabi-Siahboomi, A.R., Bowtell, R.W., Mansfield, P., Davies, M.C., Melia, C.D., 1996. Structure and behavior in hydrophilic matrix sustained release dosage forms. 4. studies of water mobility and diffusion coefficients in the gel layer of HPMC tablets using NMR imaging. Pharm. Res. 13, 376–380.

Rault, J., Gref, R., Ping, Z.H., Nguyen, Q.T., Neel, J., 1995. Glass transition temperature regulation effect in a poly-(vinyl alcohol)-water system. Polymer 36, 1655–1731.

Visavarungroj, N., Remon, J.P., 1990. Cross-linked starch as a disintegrating agent. Int. J. Pharm. 62, 125–131.

Yamamoto, T., Mukai, S.R., Nitta, K., Tamon, H., Endo, A., Ohmori, T., Nakaiwa, M., 2005. Evaluation of porous structure of resorcinol–formaldehyde hydrogels by thermoporometry. Thermochim. Acta 439, 74–79.

Zhong, Z., Sun, X.S., 2005. Thermal characterization and phase behavior of cornstarch studied by differential scanning calorimetry. J. Food Eng. 69, 453–459.

Zografi, G., Kontny, M.J., 1986. The interactions of water with cellulose- and starch-derived pharmaceutical excipients. Pharm. Res. 3, 187–194.